〔論　文〕

二酸化シリコン中の鉄超微粒子のイオン注入法による作製とその磁気的性質

林　伸行*1・森脇　隆行*2

Synthesis of Iron Nano-clusters in SiO_2 by Ion Implantation and the Magnetic Properties

Nobuyuki HAYASHI*1 and Takayuki MORIWAKI*2

Abstract:

The formation of iron nano-clusters in amorphous and crystalline SiO_2 by ion implantation was studied. The implantation of ^{57}Fe ions was performed at room temperature up to a total dose of 3.0×10^{17} ions/cm^2 with a projectile energy of 74 keV and 100 keV. It is shown by conversion electron Mössbauer spectroscopy and magnetization measurements that the clusters exhibit transitions from superparamagnetic to ferromagnetic states in the dose range of $1.0\sim1.5\times10^{17}$ ions/cm^2. This result indicates that under the same implantation conditions the clusters precipitate rapidly and effectively in SiO_2 at the smaller dose than those in α-Al_2O_3 matrices. Furthermore, we have found that Si atoms dissolve into the precipitated iron clusters in the Fe/SiO_2 nano-composites.

key words: iron clustering, SiO_2 matrix, Fe-Si alloy, Ion implantation

序

ナノ材料は現在最も活発な開発研究が行われている分野の一つである。我々は，2004年度研究報告№27で，Al_2O_3（サファイア）中にイオン注入法により合成したFe-Co合金の超微粒子の磁性について報告した。今回は，結晶質及び非晶質SiO_2（水晶，石英）中に於けるナノサイズ（10^{-9}nm）の超微粒子の形成とその物性について報告する。2酸化シリコン中の微粒子形成は，近未来の光応用，単一電子トランジスター応用などの観点から注目されている。しかし，その微粒子物性の詳細については知られていないことが多い。我々は，鉄同位体^{57}Feをイオン注入して，メスバウアー分光法で調べる手法により多くの物性を明らかにしてきた。本報告では，SiO_2における^{57}Fe超微粒子の形成に関する研究結果について述べる。次の結果が得られている；①SiO_2中には74 keVの入射エネルギーでイオン注入されたFe原子が凝集して微粒子となる効率はAl_2O_3のそれより高いこと，②この微粒子にはマトリックス中のSi原子が混入してFe-Si合金が形成されていることなど，今まで知られていなかった新たな事実を見出した。

なお，本報告は著者らが既にMRS-J誌[1]に発表済みの論文に若干のデータと考察を加えたものである。

1. INTRODUCTION

Composite systems of metal nano-clusters embedded in insulating oxide matrices have attracted much attention because of their unusual optical, electrical, and magnetic properties[2,3]. The implantation of magnetic metal ions into refractory metal oxides has

*1 機械システム工学科
*2 高知工科大学大学院工学研究科博士課程
平成17年4月14日受理

been used to form such granular films, offering potential important applications in the fields of magnetic recording media, magnetic refrigeration, medical diagnostics, and so on. We have presented that the magnetic-buried-granular layers produced by implantation of Fe ions into α-Al_2O_3 and MgO single crystals exhibit an eminent giant magnetoresistance (GMR)[4,5]. On the one hand, SiO_2 is an attractive substrate material for dispersing metal nano-clusters from the viewpoints of modern electronics, and it should be stressed that ion implantation is a technology capable of synthesizing nano-clusters with controlled size and composition and compatible with silicon device technology. Although a few studies have been reported on the characteristics of SiO_2 implanted with Fe ions at the doses over 1.0×10^{17} ions/cm^2[6,7], the physical properties of the iron clusters are still remained unclear. Therefore, it is valuable to investigate the magnetic properties in the Fe-SiO_2 composite system (Fe/SiO_2).

By combined means of conversion electron Mössbauer spectroscopy (CEMS), together with X-ray diffraction and magnetization measurements, we have investigated the formation of iron precipitates and the subsequent change in magnetic properties in the surface layers of ^{57}Fe implanted SiO_2 matrixes. It is demonstrated that the iron precipitation in the Fe/SiO_2 exhibits different properties than the iron implantation into Al_2O_3 and MgO in respect of both the rapid growth of the iron clusters and Si inclusion in the clusters.

2. EXPERIMENTAL

The sample was prepared by implantation of $^{57}Fe^+$ ions into quartz SiO_2 (a-SiO_2) substrate at a dose of (1.4~3.0) $\times10^{17}$ ions/cm^2. The energy of the projectiles was 100 keV and 74 keV with current density of a few μA/cm^2. The two energies were chosen to compare the properties of iron granules with those in Fe/Al_2O_3[5]. The implantation conditions are summarized in Table 1; e.g., the sample A was implanted with the total dose of 1.4×10^{17} ions/cm^2.

The crystalline structure of the implanted layers was characterized by glancing angle x-ray diffraction (GXRD). The GXRD patterns were measured with a glancing angle of $\theta=2.5°$, using Cu targets. CEMS was measured with a He + 4% CH_4 gas flow proportional counter, using a 740 MBq ^{57}Co source in Rh. Mössbauer spectra were analyzed by least-squares fitting with overlapping Lorentzian curves. The magnetic properties were measured with a vibrating sample magnetometer (VSM) where magnetization in granular layers were achieved by applying perpendicular and in-plane external fields H up to 15 kOe. The implantations and all measurements were performed at room temperature.

Table 1; Implantation conditions for the samples numbered as A-E. The numbers are referred in the text.

Sample Number	Matrices	100keV : [ions/cm^2]	74keV : [ions/cm^2]
A*	a-SiO_2	1.0×10^{17}	0.4×10^{17}
B	a-SiO_2	0	1.5×10^{17}
C	a-SiO_2	3.0×10^{17}	0
D	c-SiO_2	0	1.5×10^{17}
E	Al_2O_3	1.5×10^{17}	0

* It is noted that the total dose of the sample A is 1.4×10^{17}/cm^2.

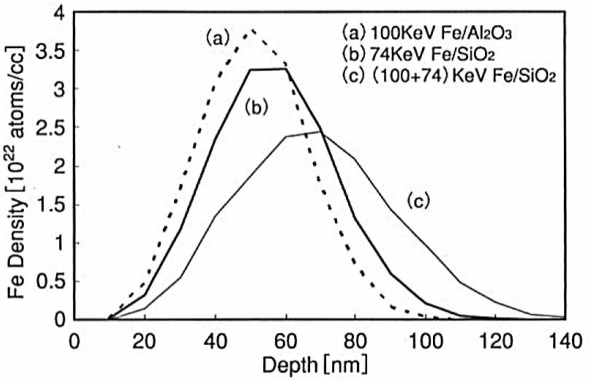

Fig. 1; Fe ions distribution calculated from TRIM code for the sample E (Fe/Al_2O_3), sample B (Fe/SiO_2), and sample A (Fe/SiO_2)

Fig. 1 shows simulation curves of the Fe distribution calculated by the TRIM code for the samples A, B and E. It is noted in the figure that the ion distribution with 74 keV implantation in SiO_2 substrate is comparable with 100 keV ions in Al_2O_3 and that the implantation with two stages of 100 keV and 74 keV (sample

A) offers two third peak concentration of the 74 keV implantation (sample B) because of deeper incorporation of Fe ions into the SiO_2 matrices due to the lower density than in Al_2O_3.

3. RESULTS AND DISCUSSIONS

Fig. 2 shows typical GXRD pattern from the implanted layers of SiO_2 substrates, together with that in Al_2O_3 for comparison. A rather sharp peak appears at about $2\theta=45^\circ$ corresponding to the diffraction from bcc α-Fe (110) planes. The GXRD peaks were analyzed by the least-squares fitting assuming Gaussian curves, $I(x)=\frac{1}{\sqrt{2\pi}\sigma}\exp\left(-\frac{x^2}{2\sigma^2}\right)$, where $x=\theta-\theta p$, θp is the diffraction angle and σ is a variance of Gaussian. The obtained lattice parameters are summarized in Table 2. The lattice parameters of Table 2 are comparable with the value of 0.287 nm in bulk α-iron, but the results for the samples B and D with higher doses indicate the shrinkage of the cluster's lattice. We have also performed implantation in crystalline SiO_2 (c-SiO_2) substrate, in order to investigate whether the crystalline structure of the matrix affects the precipitation of α-iron. The results from Fig. 2 and Table 2 show that there appears to be a little difference between the precipitation in a-SiO_2 and in c-SiO_2, suggesting that the implanted iron may precipitate through the amorphized matrix. On the other hand, it

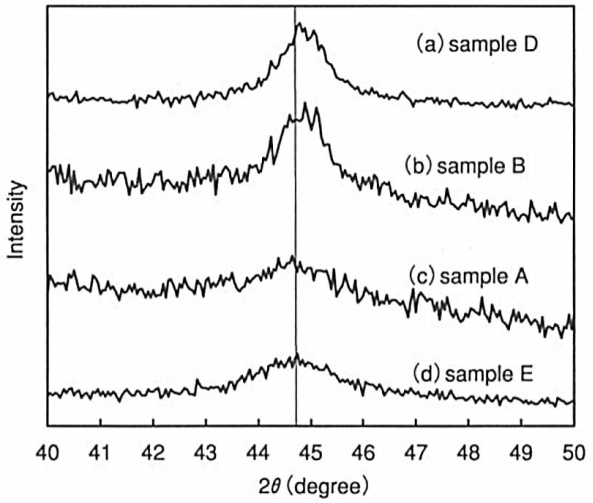

Fig. 2; GXRD patterns from the implanted layers of the sample A (Fe/SiO_2), sample B (Fe/SiO_2), sample D (Fe/SiO_2), and sample E (Fe/Al_2O_3). The vertical line indicates the (110) diffraction angle of bulk iron.

Table 2; GXRD parameters of Fe/Si granules obtained from the analysis of XRD curves in Fig. 2.

Granules : Dose [ions/cm²]	2θ	Peak width	Lattice parameter [nm]	Cluster diameter [nm]
1.4×10^{17} (sample A)	44.8°	1.01°	0.286	6
1.5×10^{17} (B)	44.9°	0.44°	0.284	15
1.5×10^{17} (D)	44.9°	0.51°	0.284	13
1.5×10^{17} (E)	44.7°	0.88°	0.286	7

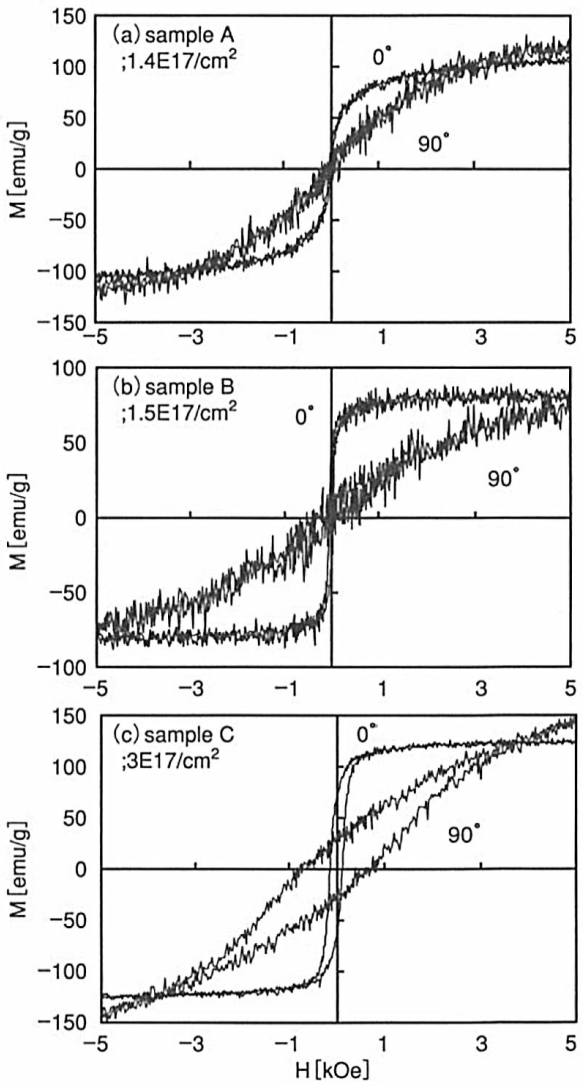

Fig. 3; Magnetization curves taken from iron implanted a-SiO_2. sample A with a dose of $(1.0+0.4)\times10^{17}$ ions/cm², sample B with 1.5×10^{17} ions/cm², and sample C with 3.0×10^{17} ions/cm²

is noted that at a dose of 1.5×10^{17} ions/cm^2 the size of the nano-particles in the SiO_2 is approximately twice as large as that in Al_2O_3 matrix.

Fig. 3 shows magnetization curves measured for the samples implanted to high doses in SiO_2 matrices. The curves with thick and thin lines denote the magnetization when applying in-plane and perpendicular fields, respectively. We can hardly see the magnetic hysteresis loop and the saturation of magnetization in the sample A (Fig. 3a). It indicates for the most nano-clusters to be superparamagnetic. In the paramagnetic state the magnetization M is expressed as a function of external field H by Langevin function, i.e., $M(H, T)=Ms\left[\coth\left(\frac{\mu_i H}{kT}\right)-\left(\frac{kT}{\mu_i}\right)^{-1}\right]$, where Ms is the saturation of magnetization, and μ_i is the magnetic moment of Fe atoms. The magnetization curve for the sample A was confirmed to be induced as the Langevin function evolves. While the sample B with a dose of 1.5×10^{17} ions/cm^2 exhibits the curves with a superposition of the superparamagnetism and ferromagnetism, for the sample C the hysteresis loops are more eminent for both in-plane and perpendicular fields, indicating intensively ferromagnetic characteristic. The results show that the difference between the curves of the samples A and B is caused by the difference of Fe density in the implanted layer as shown in the simulation curves in Fig. 1 and that the nano-clusters grow in the size with increasing dose. The difference between in-plane and perpendicular magnetization indicates that the average of the easy directions of magnetization are in the implanted plane. It is suggested that the most probable source of the magnetic anisotropy is shape anisotropy, i.e., the iron nano-particles are in the shape of oblate ellipsoids[8]. The consideration on the anisotropy is consistent with CEMS measurements whose spectrum shows that the intensities of the second and fifth lines of the magnetic splitting are larger than those of the outer lines as shown in Fig. 4. The values of saturation magnetization in Fig. 3 are much higher than those of Fe/SiO_2 granules reported by Ding' et al.[6] but still lower than that of bulk iron (~220 emu/g), while the coercivity estimated from the sample C is obtained as 127 Oe and is much higher than that of bulk iron (~10 Oe), which is considered to be caused by the uniaxial anisotropy.

Mössbauer spectroscopy is useful to elucidate the physical states of the implanted irons through the measurement of hyperfine parameters. Fig. 4(a) shows a CEM spectrum from the SiO_2 samples implanted to a total doses of 1.4×10^{17} ions/cm^2 where the clusters' size has been estimated as 6 nm. The central part of the spectrum was fitted with the assumption of overlapping Lorenzians which consist of one single line and three quadrupole doublets from ferric and two forms of ferrous irons. The doublets assigned to the ionic forms of Fe^{3+} and Fe^{2+} are supposed to arise from the iron oxides in complex form[7]. The single line peaked near zero velocity can be ascribed to metallic α-iron aggregates (Fe^0) that exhibit superparamagnetic characteristics due to its small size in nanometer scale[8]. A set of magnetic sextet lines was added to fit the fringe on the central peaks in Fig. 4. The appearance of the sextet suggests that among the superparamagnetic granules the ferromagnetic nano-particles are evolved in the dispersion of Fe/SiO_2 composites even at such a low dose as 1.4×10^{17} ions/cm^2.

It is shown in Fig. 4(b) that the magnetic sextets, i.e., ferromagnetic component of Fe^0, appear clearly at the expense of superparamagnetic Fe^0 components for the samples with an increased dose of 1.5×10^{17} ions/cm^2. The result reveals that most of the iron nano-particles precipitate in ferromagnetic state due to the size increase with increasing dose. On the other hand, we have shown that in Fe/Al_2O_3 composites the critical size of Fe^0 granules where the superparamagnetic relaxation is blocked at room temperature is achieved at the dose of $(1.5\sim2.0)\times10^{17}$ ions/cm^2. Thus, the ferromagnetic clusters appear at the smaller dose by 0.5×10^{17} ions/cm^2 than in Fe/Al_2O_3, indicating that the implanted irons aggregate rapidly and effectively in the SiO_2 matrixes. To be excellent, the result is consistent with the results of XRD and VSM measurements.

Fe-Si alloys have been the materials of great interest for many decades and alloys of the low silicon

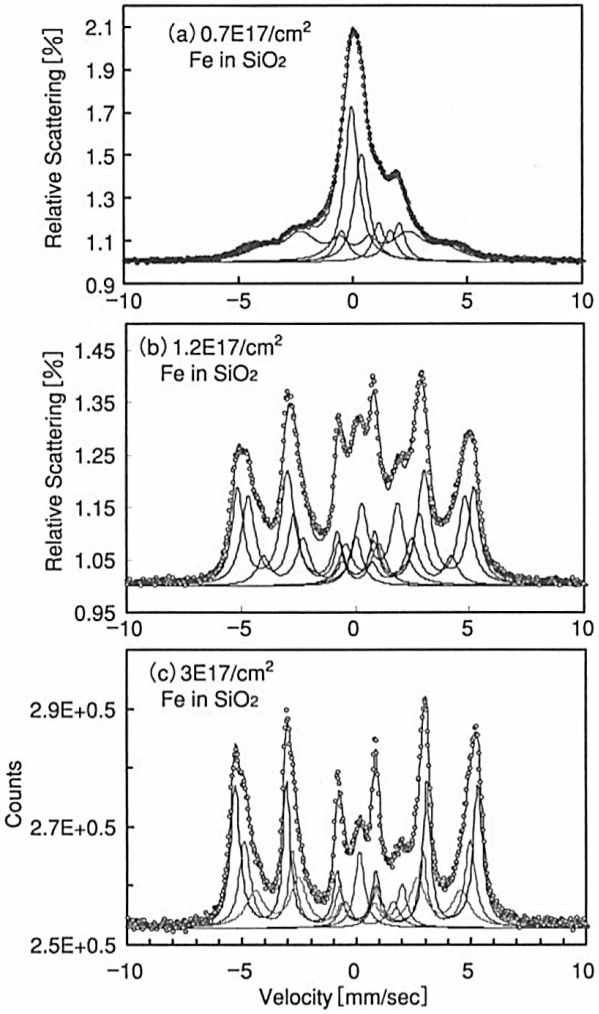

Fig. 4; CEM spectra of the Fe/SiO_2 granules from iron implanted a-SiO_2; (a) with a dose of 0.7×10^{17} ions/cm², (b) with 1.2×10^{17} ions/cm² and (c) with 3.0×10^{17} ions/cm² (sample C)

Table 3; Mössbauer parameters of iron nano-particles present in implanted Fe/SiO_2 samples, obtained from the spectrum of Fig. 4(b). *IS* is the isomer shift and B_{hf} the internal field.

Sample preparation	Hyperfine parameters	Iron site 1	Site 2	Site 3
Implanted Fe/a-SiO_2	B_{hf} [kOe]	321	296	256
	$B_{hf,n}/B_{hf\ 1}$*	1.00	0.920	0.797
	I.S. [mm/s]	0.026	0.057	0.084
Bulk Fe-Si alloys	$B_{hf\ 1}/B_{hf\ Fe}$*	1.00	0.917	0.834
	I.S. [mm/s]	0.01	0.03	0.09

* Column shows the B_{hf} change relative to the site 1.

region have been well investigated for practical uses. It is well known that the disordered alloys with 0-10 at. % Si show separate internal magnetic fields, B_{hf}, due to the iron atoms with different nearest neighbours of solute Si and that the chemical isomer shift in the alloys increases regularly with increase in the nearest neighbour Si atoms. The spectrum in Fig. 4 clearly exhibits ferromagnetic splitting with three resolvable internal magnetic fields whose pattern is very similar to that observed for disordered Fe-Si bulk alloys[10]. The hyperfine parameters obtained from the analysis for the ferromagnetic iron clusters are summarized in Table 3. The B_{hf}, value of 321 kOe for the site 1 is close to that of bulk iron, 330 kOe, and the difference of 10 kOe is caused by collective excitation of the nano-particles[11]. It is clearly demonstrated that the re-lative change in both internal fields and isomer shifts for the sites 2 and 3 are in good agreement with those measured in bulk alloys. Therefore, the three sites are considered to correspond to the Fe atoms which have 8, 7 and 6 nearest-neighbor Fe atoms; i.e., the latter two cases correspond to one and two Si atoms substitution for the iron sites in the bcc lattice. The Si concentration is estimated to be in the range of 5~10 at. %, judging from the intensity of the site 3[10]. The Si atoms are supposed to be taken part in the iron precipitation from SiO_2 matrix during collision cascades of ion implantation. The alloy formation is consistent with the result of XRD measurements, i.e., the decrease in lattice parameters of the Fe/SiO_2 composite, because the lattice constant decreases by 0.3% with alloying of 10 at. % Si. Although the Si inclusion is reasonable from thermodynamic inspections taking account of bond strength, there has not been reported any experimental observation. It is noteworthy that in the case of Fe/Al_2O_3 granules the iron clusters never include Al from the matrices atoms during ion implantation because the ferromagnetic clusters are characterized by only one internal magnetic field[12].

We would expect a significant GMR effect in the Fe/SiO_2 granular layers prepared by ion implantation to the dose of 1.4×10^{17} ions/cm² since an amount of

superparamagnetic nano-particles exists there, and actually the magnetization measured by VSM was comparable to that observed in the Fe-implanted Al_2O_3 granules[4]. MR ratios in the iron granules prepared by implantation was observed to be 7.5% for Fe/Al_2O_3 and 3.5% for Fe/MgO for H=12 kOe[4,5]. Furthermore, the MR ratio in the granular Fe/SiO_2 films prepared by rf sputtering was observed to be (2-3)%, depending on Fe content[13]. However, the MR ratio in the implanted Fe/SiO_2 was observed to be 1% at most for H=12 kOe. The difference of GMR evolution could be attributed to the insufficient dispersion of Fe nano-clusters in the implanted layer. It is likely that the bigger size of the nano-clusters causes the larger separation between the clusters in Fe/SiO_2 than in Fe/Al_2O_3 and sputtered Fe/SiO_2 film, and leads to the decrease of electron tunneling probability and then the GMR effects. We can say that the rapid growth of iron precipitation in the implanted Fe/SiO_2 layers causes the lowering of the GMR effect. The peculiar growth process of the nano-clusters in the Fe/SiO_2 granules is reasonable from a viewpoint of thermodynamics and will be discussed in the next report, together with a new result in the innovation of the alloy nano-particles synthesized in SiO_2 matrices[14].

4. CONCLUSION

Ion implantation was used to modify magnetic properties in the surface layers of amorphous SiO_2 and the layers were investigated by combined methods of X-ray diffraction, magnetization measurement and Mössbauer spectroscopy. The prepared granules exhibit from superparamagnetic to ferromagnetic transition at a smaller dose than that in Fe/Al_2O_3, which means rapid growth of the nano-clusters in the implanted SiO_2 matrix. Most of the nano-particles are in ferromagnetic state at the dose of 1.5×10^{17} ions/cm^2. We have found for the first time, to our knowledge, that an amount of Si atoms are mixed in the iron precipitation during ion implantation and Fe-Si alloys are formed in the nano-clusters.

ACKNOWLEDGMENTS

A part of this study was financially supported by the Yoshida Foundation for the Promotion of Learning and Education (Daiden Corp., Kurume-shi).

REFERENCES

[1] T. Moriwaki, N. Hayashi, I. Sakamoto, H. Tanoue, T. Toriyama, and H. Wakabayashi, Trans. Mater. Research Soc. Jpn., **29**, 607-610 (2004).

[2] C.E. Vallet, C.W. White, S.P. Withrow, J.D. Budal, L.A Boatner, K.D. Sorge, J.R. Thmpson, K.S. Beaty and A. Meldrum, J. Appl. Phys., **92**, 6200-04 (2002).

[3] G.L. Zhang and H. Pattyn, Hyperfine Interact., **113**, 165-181 (1998)

[4] N. Hayashi, I. Sakamoto, H.Tanoue, H.Wakabayashi, and T. Toriyama, Hyperfine Inter., **158/159**, 193-97 (2003).

[5] N. Hayashi, I. Sakamoto, T. Toriyama, H. Wakabayashi, T. Okada, and K. Kuriyama, Surface and Coating Techno., **169/170**, 540-43 (2003).

[6] Xing-zhao Ding, B.K. Tay, X.Shi, M.F. Chiah, W. Y. Cheung, S.P. Wong, J.B. Xu, and I.H. Wilson, J. Appl. Phys., 88, 2745-49 (2000).

[7] A. Perez, M. Treilleux, T. Capra, and D.J. Criscom, J. Mater. Res., 2, 910-917 (1987).

[8] H. Wakabayashi, T. Hirai, T. Toriyama, N. Hayashi, and I. Sakamoto, Phys. Status Solidi A, 94, 515-520 (2002).

[9] C.J. McHargue, P.S. Sklad, C.W. White, G.C. Farlow, A. Perez, and G. Marest, J. Mater. Res., **6**, 2145-2159 (1991)

[10] M.B. Stearns, Phys. Rev.. **129**, 1136-1144 (1963)

[11] F. Bodker and S. Morup, Hyperfine Interact., **93**, 1421-25 (1994)

[12] N. Hayashi, I. Sakamoto, H. Tanoue, H. Wakabayashi, and T. Toriyama, J. Appl. Phys., **94**, 2597-601 (2003).

[13] S. Honda, T.O. Okada, M. Nawate, and M. Tokumoto, Phys. Rev., **56**, 14556-573 (1997).

[14] N. Hayashi, I. Sakamoto, T. Moriwaki, H.Wakabayashi, and T. Toriyama, J. Magn. Magn. Mater., **290/291**, 98-101 (2005).